

# Ultrafast laser-induced phase transitions in tellurium

*S. I. Ashitkov, M. B. Agranat<sup>1)</sup>, P. S. Kondratenko, S. I. Anisimov, V. E. Fortov,  
V. V. Temnov<sup>+</sup>, K. Sokolowski-Tinten\*, B. Rethfeld\*, P. Zhou\*, D. von der Linde\**

*Institute of High Energy Density, Joint Institute for High Temperatures RAS, 127412 Moscow, Russia*

<sup>+</sup>*Institute of Applied Physics RAS, 603600 Nizhny Novgorod, Russia*

<sup>\*</sup>*Institute for Laser and Plasma Physics, University of Essen, 45117 Essen, Germany*

Submitted 2 September 2002

We present experimental investigations of ultrafast phase transitions in tellurium following excitation with an intense femtosecond laser pulse. Femtosecond time-resolved polarization-sensitive microscopy is used to monitor the temporal evolution of the optical anisotropy (birefringence) of the irradiated material. The decay of the optical anisotropy associated with the loss of order in crystalline tellurium is fluence dependent and occurs within 0.5–3 ps.

PACS: 63.90.+t, 78.90.+t

Ultrafast laser processing of materials, especially metals and semiconductors, is a field of condensed-matter physics and material science that has developed rapidly over the last few years. It has proved to be of considerable interest for both applied and fundamental research for a variety of reasons, which are discussed extensively in the literature [appropriate reference]. An important application of ultrashort laser pulses is connected with the study of ultrafast phase transitions. In our previous work [1] we studied experimentally ultrafast changes of order of monocrystalline graphite under irradiation by a femtosecond laser pulse using a new experimental technique that exploits the optical anisotropy of the crystal.

In this letter we present the results of a similar study, performed on samples of monocrystalline tellurium. The experiments are performed with a chirped-pulse-amplified Ti:sapphire laser system (100 fs pulse duration), using time-resolved polarization sensitive optical microscopy [1]. The sample surface is excited by an intense s-polarized pump laser pulse at 800 nm (angle of incidence 45°) and probed by a weak time-delayed p-polarized probe laser pulse at 400 nm (normal incidence). Snapshots of the laser-excited surface are recorded by a digital CCD-camera. Further details of the technique can be found in [1].

The (100) surface of monocrystalline tellurium contains the optical anisotropy axis. Rotating the sample around the surface normal allows variation of the angle  $\varphi$  between the anisotropy axis and the polarization vector of the probe pulse. In this way the ordinary re-

flectivity  $R_o$  ( $\varphi = 90^\circ$ ), extraordinary reflectivity  $R_e$  ( $\varphi = 0^\circ$ ) as well as the so-called “anisotropic” reflectivity component  $R_{cr}$  ( $\varphi = 45^\circ$ ) [1] can be measured:

$$R_o = \left| \frac{n_o - 1}{n_o + 1} \right|^2, \quad R_e = \left| \frac{n_e - 1}{n_e + 1} \right|^2, \quad R_{cr} \approx \frac{|2\delta|^2}{|n + 1|^4},$$

where  $n_o$  and  $n_e$  are the complex refractive indices for ordinary and extraordinary polarization;  $\delta = (n_e - n_o)/2$ , and  $n = (n_e + n_o)/2$ .

The complex indices of refraction for unexcited tellurium are [2]: for the pump ( $\lambda = 800$  nm)  $n_o = 5.84 - 1.06i$ ,  $n_e = 6.73 - 2.89i$ , for the probe ( $\lambda = 400$  nm)  $n_o = 2.37 - 3.29i$ ,  $n_e = 2.22 - 3.96i$ . The skin-depths ( $\mu = \lambda/4\pi \text{Im } n$ ) are  $\mu_o = 60$  nm,  $\mu_e = 22$  nm for the pump and  $\mu_o = 10$  nm,  $\mu_e = 8$  nm for the probe. Thus, the skin-depth at the probe wavelength is always less than the skin-depth of the pump pulse.

In Fig.1a snapshots of the transient changes of the anisotropic reflectivity in the laser irradiated area are presented. Corresponding spatial cross sections, representing the fluence dependence of the “anisotropic” reflectivity component at a given time instant are depicted in Fig.1b. From Fig.1b it can be seen that during the first few picoseconds the intensity of the “anisotropic” reflectivity component drops drastically in the center of the focal spot (maximum fluence) indicating a corresponding loss of the optical anisotropy, which is interpreted as a loss of crystalline order [1] in the excited surface layer. The threshold fluence with respect to the change of anisotropic reflection is about  $F \approx 15$  mJ/cm<sup>2</sup> (a study of melting near the threshold fluence is a subject of our future researches, as it demands modernization of an experimental technique). The recovery

<sup>1)</sup>e-mail: utpr@iht.mpei.ac.ru

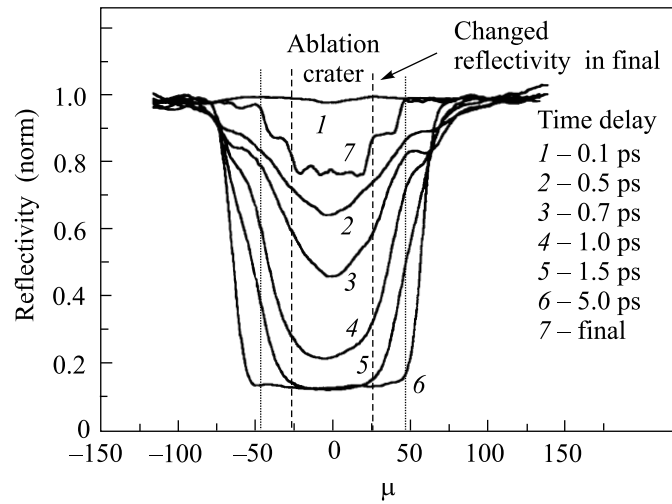


Fig.1. Transient snapshots (a) and profiles (b) of the "anisotropic" reflectivity  $R_{cr}$  of the excited Te surface for different pump-probe time delays for a pump peak fluence of  $66 \text{ mJ/cm}^2$

of the anisotropic reflectivity back to nearly the initial value indicates crystallization upon resolidification. This process is much slower and takes a few nanoseconds.

Fig.2 shows the temporal evolution of the ordinary, extraordinary and "anisotropic" reflectivities for differ-

ent excitation fluences above the melting threshold. It is clear to see that the decay time of the "anisotropic" reflectivity component coincides with the time at which the ordinary and extraordinary reflectivities become equal. Within a few picoseconds the optical anisotropy for the presented fluences disappears, whereas the isotropic reflectivity reaches a constant value. We interpret the observed rapid loss of optical anisotropy and the existence of a stationary isotropic reflectivity at later times to be due to the formation of a liquid surface layer with a thickness larger than the penetration depth of the probe pulse. Thus the decay time of the optical anisotropy may be referred to as the *melting time*.

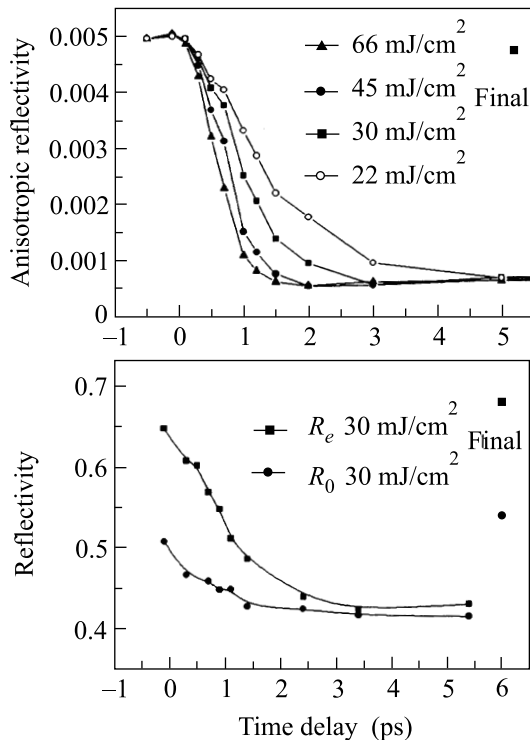


Fig.2. Temporal evolution of the "anisotropic" (a), ordinary ( $R_o$ ) and extraordinary ( $R_e$ ) (b) reflectivity components for different laser fluences above the melting threshold

Fig.2a shows the temporal evolution of the anisotropic reflectivity component for different laser fluences and aims to demonstrate the pronounced dependence of the *melting time* on the incident laser fluence. The melting time derived by a simple exponential fit of the measured time dependencies in Fig.2a is plotted in Fig.3 as a function of the laser fluence. For laser fluences above  $45 \text{ mJ/cm}^2$ , which is approximately three times the melting threshold, the melting process occurs essentially in less than one picosecond. For laser fluences closer to the melting threshold the melting time increases up to a few picoseconds.

In order to provide a physical interpretation of the results of our optical measurements we have analyzed the optical properties of a thin film of liquid tellurium on a crystalline tellurium substrate. The optical constants of liquid tellurium were determined by means of time-resolved interferometry [3]. This technique allows for femtosecond time-resolved measurements of changes (relative to unexcited tellurium) in both the amplitude

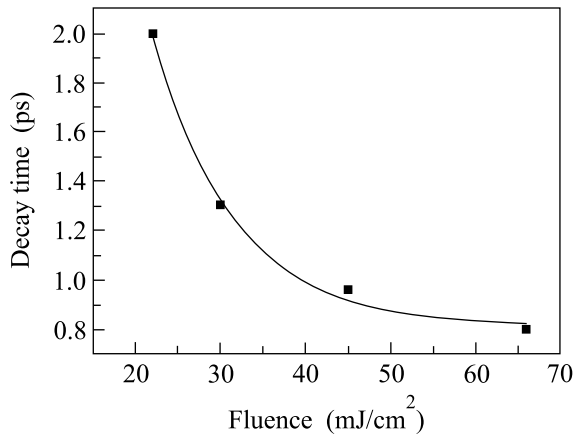


Fig.3. Melting time as function of laser fluence (see text for details)

and the phase of the reflected probe light. We have performed the interferometric measurements for sufficiently high fluences at long delay times up to a few nanoseconds, to assure that the laser-melted layer of liquid tellurium has a thickness larger than the skin-depth of the probe. Taking the optical constants of crystalline tellurium at  $\lambda = 400$  nm as reference values and using the Fresnel formulas we determine the complex index of refraction for liquid Te at our probe wavelength as:  $n_{\text{liquid Te}} = 2.6 - 2.1i$ . The reflectivities obtained with the measured optical constants for liquid Te are in good agreement with previously reported results [4]. It is important to note that at  $\lambda = 400$  nm the skin-depth in the melt ( $\mu_{\text{liquid Te}} = 15$  nm) is larger than in the crystalline solid ( $\mu_o = 10$  nm,  $\mu_e = 8$  nm), but still less, than the skin-depth in the solid for the pump.

Let us discuss now the physical mechanisms of melting operative in tellurium. More precisely, we wish to distinguish between three different possible melting pathways: non-thermal melting, bulk thermal melting via homogenous nucleation and heterogeneous thermal melting. Non-thermal melting describes a transition to the liquid phase, which is driven by an electronically induced instability of the lattice upon excitation of sufficiently dense electron-hole plasma [5], and which has been extensively studied in covalently bonded semiconductors. This kind of melting can be extremely fast (100 fs time-scale) because it does not require heating of the lattice prior to the phase transition.

The borderline between thermal and non-thermal processes is determined by the time needed for the energy transfer from the primarily excited electronic system to the lattice. This time can be estimated using the two-temperature model [6, 7]. For femtosecond laser excitation, the characteristic time of temperature equilibration is  $\tau = c_e c_i / \alpha (c_e + c_i)$  [8], where  $c_e$  and  $c_i$  are the

heat capacities of the electrons and lattice, respectively, and  $\alpha$  is the electron-phonon coupling constant. In tellurium the heat capacity of the electrons is very small [9], thus the characteristic time for lattice heating is approximately given by  $\tau \approx (c_e / \alpha)$ . If typical values for  $\alpha$  in metals are applied (unfortunately  $\alpha$  is not known for the specific case of tellurium) thermalization times of 1 ps or less are derived. Therefore, for the largest pump fluences studied in this work ( $F > 45$  mJ/cm<sup>2</sup>) the observed melting time is comparable to the characteristic time of lattice heating and it is not possible to distinguish between non-thermal and thermal melting processes.

However, for lower fluences melting needs longer times ( $> 1$  ps) and can be regarded as thermal in nature. Usually it is assumed that melting occurs *heterogeneously* starting at the surface where no nucleation barrier exists and proceeds into the bulk with a velocity ultimately limited by the speed of sound. It follows from the above analysis of the optical constants that the observation of stationary isotropic optical properties requires a liquid layer with a thickness of at least 15 nm. The sound velocity in solid tellurium is about  $c_s \approx 2000$  m/s [9] which sets a *lower* limit for the time of heterogeneous melting of about 7–10 ps. Therefore, for the fluence range presented in this work, heterogeneous melting can be excluded, although, it may occur for fluences very close to the melting threshold.

In order to explain melting times of just a few picoseconds, which are observed in this work, we invoke the model of thermal melting via *homogenous* nucleation [10]. This model describes the formation of liquid nuclei in the bulk of an overheated solid, i.e. *after* the hot laser-excited electrons have thermalized with the initially cold lattice via electron-phonon coupling. We would like to stress that the formation of liquid nuclei inside the bulk is generally less probable than the formation of a liquid layer at the free surface. However, under strong superheating the melting over the skin-depth by homogeneous nucleation can be in fact faster than the melting due to the propagation of a solid-liquid interface from the surface into the bulk of the material. In particular, it was shown recently [10] that for high superheating, corresponding to excitation fluences sufficiently above the melting threshold, the melting time by thermal homogeneous nucleation is essentially limited by the time needed for energy thermalization.

In summary, we have applied ultrafast time-resolved optical anisotropy measurements to study structural transitions in femtosecond laser-excited mono-crystalline tellurium. The presented data indicate

that in this material melting may occur by thermal homogeneous nucleation.

The authors would like to thank S.V.Petrov from ITP RAS for tellurium samples.

This work was supported by NATO Grant SA(PST.CLG # 975059) and the Forschungspool of the University of Essen (V.T.).

1. S. I. Ashitkov, M. B. Agranat, P. S. Kondratenko et al., *Pis'ma v ZhETF* **75**, 96 (2002).
2. *Handbook of Optical Constants of Solids*, Ed. E. D. Palik, Academic, Orlando, 1985.
3. V. V. Temnov, K. Sokolowski-Tinten, and D. von der Linde, to be published.
4. L. A. Silva and M. Cutler, *Phys. Rev.* **B42**, 7103 (1990).
5. J. A. van Vechten, R. Tsu, and F. W. Saris, *Phys. Lett.* **A74**, 422 (1979).
6. S. I. Anisimov, B. L. Kapeliovich, and T. L. Perel'man, *Sov. Phys. JETP* **39**, 375 (1974).
7. B. Rethfeld, A. Kaiser, M. Vicanek, and G. Simon, *Phys. Rev.* **B65**, 214303 (2002).
8. J. J. Klossika, U. Gratzke, M. Vicanek, and G. Simon, *Phys. Rev.* **B54**, 10277 (1996).
9. I. S. Grigorev and E. Z. Mejlikhov, *Fizicheskie Velichini*, Moskau, Energoatomizdat, 1991.
10. B. Rethfeld, K. Sokolowski-Tinten, D. von der Linde, and S. I. Anisimov, *Phys. Rev.* **B65**, 092103 (2002).